Alexandria Engineering Journal (2017) 56, 383–394

HOSTED BY

Alexandria University

Alexandria Engineering Journal

www.elsevier.com/locate/aej
www.sciencedirect.com

ORIGINAL ARTICLE

Lateral motion control of skid steering vehicles using full drive-by-wire system

Ossama Mokhiamar [a,b,*], Semaan Amine [a]

[a] Beirut Arab University, Faculty of Engineering, Mechanical Engineering Department, P.O. Box 11-5020, Riad El Solh, Beirut 1107-2809, Lebanon
[b] Alexandria University, Faculty of Engineering, Mechanical Engineering Department, El-Chatby, Alexandria 21544, Egypt

Received 22 December 2016; revised 16 February 2017; accepted 13 March 2017
Available online 1 April 2017

KEYWORDS

Vehicle dynamics;
Traction control;
Nonlinear control;
Skid steering vehicles

Abstract This paper introduces a control system to stabilize the motion of skid steering vehicles, extends their stability limit and makes their handling performance similar to that of the conventional two-wheel steering vehicle. For this purpose, the yaw rate response of the two degree of freedom (2DOF) linear model of the conventional two-wheel steering vehicle is chosen as a model response. The model following control theory is used to introduce the direct yaw moment needed to stabilize and steer the skid steering vehicle. The direct yaw moment has been split into the four tires based on two methods. The first method is based on a simple distribution technique (SD), whereas the second method is based on an independent distribution technique (ID) where the four wheels can be driven individually using a full drive-by-wire system. A comprehensive nonlinear dynamic model of the skid steering vehicle has been simulated using Matlab/Simulink in order to examine the effectiveness of the proposed control system. The results of both open and closed loop tests show that the proposed control system has a significant effect on stabilizing the lateral motion of skid steering vehicles as well as improving their handling characteristics.

1. Introduction

Over the past decade, a few researches have addressed the increase in the stability limit of conventional two-wheel steering vehicles based on an optimal distribution of both longitudinal and lateral tire forces. Suzuki et al. [1] studied feedforward types of tire force distribution controls for full drive-by-wire electric vehicles based on two strategies. The first strategy was to minimize the tire workload whereas the second strategy was to minimize the tire energy dissipation. The effect of the control system was investigated experimentally on a proving ground where it was concluded that the first strategy has a great influence on the vehicle stability. Goodarzi and Mohammadi [2] designed an integrated control of three layers for improving the stability and the fuel economy of a 4-wheel-drive hybrid vehicle. One of the three layers was to determine the optimum values of longitudinal and lateral forces of the four tires that allow achieving a desired vehicle response.

* Corresponding author at: Beirut Arab University, Faculty of Engineering, Mechanical Engineering Department, P.O. Box 11-5020 Riad El Solh, Beirut 1107-2809, Lebanon.
E-mail addresses: ossama.mokhiamar@bau.edu.lb (O. Mokhiamar), s.amin@bau.edu.lb (S. Amine).
Peer review under responsibility of Faculty of Engineering, Alexandria University.

http://dx.doi.org/10.1016/j.aej.2017.03.024

Nomenclature

a	distance from the mass center of the vehicle to front axle
a_x	longitudinal acceleration
a_{xdes}	traction/braking command from the driver
a_y	lateral acceleration
A	stability factor
b	distance from the mass center of the vehicle to rear axle
B_{pitch}	suspension pitch damping coefficient
B_{roll}	suspension roll damping coefficient
C_f	cornering stiffness of front wheel
C_r	cornering stiffness of rear wheel
dr	distribution ratio of the direct yaw moment
F_{xi}	friction force in the longitudinal direction of wheel i (i = 1–4)
F^*_{xi}	required longitudinal force at wheel i (i = 1–4)
F_{yf}	linear lateral force produced by front wheels
F^*_{yf}	estimated lateral force produced by front wheels
F_{yi}	friction force in the lateral direction of wheel i (i = 1–4)
F_{yr}	linear lateral force produced by rear wheels
F^*_{yr}	estimated lateral force produced by rear wheels
F_{zi}	estimated vertical load of wheel i (i = 1–4)
g	gravity acceleration
G_R	yaw rate gain
h_s	sprung mass height
I_x	mass moment of inertia about the x-axis
I_y	mass moment of inertia about the y-axis
I_z	yaw moment of inertia
J_i	moment of inertia of wheel i (i = 1–4)
k	time constant
k_f	lateral weight-shift distribution on the front wheel
k_r	lateral weight-shift distribution on the rear wheel
K_{pitch}	suspension pitch stiffness
K_{roll}	suspension pitch stiffness
M_z	direct yaw moment control
M_{zf}	direct yaw moment to be generated from front wheels
M_{zr}	direct yaw moment to be generated from rear wheels
p	pitch angular velocity of the vehicle about the y-axis
$\dot{p}$	pitch angular acceleration of the vehicle about the y-axis
q	roll angular velocity of the vehicle about the x-axis
$\dot{q}$	roll angular acceleration of the vehicle about the x-axis
r	steering gear ratio
R	wheel radius
s	Laplace transform
S	sliding surface
t	vehicle tread
T_i	traction/braking torque at wheel i (i = 1–4)
V	speed of the vehicle
V_x	speed of the vehicle in the longitudinal direction
$\dot{V}_x$	acceleration of the vehicle in the longitudinal direction
V_y	speed of the vehicle in the lateral direction
$\dot{V}_y$	acceleration of the vehicle in the lateral direction
W	vehicle weight
W_s	vehicle sprung weight
x	vehicle longitudinal direction
y	vehicle lateral direction
z	vehicle vertical direction
α	sideslip angle of the vehicle
α_{es}	estimated vehicle sideslip angle
$\dot{\alpha}$	time derivative of sideslip angle
γ	yaw rate of the vehicle
γ_{ss}	steady state yaw rate response
$\dot{\gamma}$	yaw acceleration of the vehicle
ζ	damping factor
θ	pitch angle of the vehicle
μ	sum of squared normalized longitudinal forces produced at the four wheels
φ	roll angle of the vehicle
ψ	driver's steering wheel angle
ω_i	angular velocity of wheel i
ω_n	natural frequency

The simulation results showed noticeable improvements on the stability and fuel consumption of the vehicle. Following the driver command, Wang et al. [3] found the optimum tire forces to follow a given target path. Computer simulations were conducted to validate the effectiveness of the proposed control. In the simulation, a 7 degrees of freedom vehicle model was used while the magic formula model was used to detect the tire forces. Based on proportional, integral and derivative (PID) control theory, Kim et al. [4] determined the yaw moment required to stabilize the lateral vehicle motion of rear wheel drive electric vehicles. Then, they distributed the yaw moment to the wheels in order to calculate the needed longitudinal tire force by taking into account the desired longitudinal force according to the driver input through the accelerator pedal. CarSim software was used to verify the effectiveness of the proposed method. During cornering with high speed, the simulation results showed a saving in the electric energy in addition to an improvement of the vehicle stability. Naraghi et al. [5] presented an integration of the vehicle longitudinal and lateral motion control in which the tire forces were distributed based on an adaptive optimal approach. In the proposed system, each tire was assumed to be steered and driven and/or braked individually. Digital simulations were executed based on a comprehensive nonlinear vehicle model. The results proved the positive influence of the proposed control. Mokhiamar [6] and Mokhiamar and Abe [7] proposed an optimum distribution of lateral and longitudinal tire forces based on minimizing the tire workload. The 2DOF state variables, yaw rate and sideslip angle, were chosen as desired responses for the model following control. A comprehensive nonlinear vehicle model was used to predict the dynamics of the controlled vehicle via computer simulations. The results

of the simulations showed a great effect of the control system on the vehicle handling characteristics. Once again, the idea of minimizing the tire workload was presented by Ono et al. [8] based on nonlinear optimization technique to find out the steering angle and traction/braking torque at the four wheels.

Skid steering vehicles are mainly used in off-road vehicles in addition to some four and six wheeled vehicles. On the other hand, a few skid steering vehicles run at medium/high speed. Instead of turning the vehicle by steering the front wheels, as in the conventional two-wheel steering vehicle, the wheels on each side can be driven at various speeds to turn the skid steering vehicle. This can be achieved by intentionally applying traction/braking force on the wheels to produce the direct yaw moment needed to turn the vehicle. Accordingly, the mechanical steering system will be eliminated which results in more interior space. The caster wheel effect will be eliminated as well. As stated by Sasaki and Abe [9], it is not easy to drive skid steering vehicles especially for drivers who are used to drive conventional two-wheel steering vehicle. This is due to the over-steer characteristics of skid steering vehicles mainly when the vehicle speed increases.

It is noteworthy that a very few studies were conducted to find out the proper distribution of the longitudinal forces that should be produced at the four wheels in order to stabilize the motion of skid steering vehicles. Sasaki and Abe [10] proposed an approximate first order lag of the yaw rate response of the 2DOF linear vehicle model as a target response for the model following control. The direct yaw moment control, needed to be generated from the four wheels in order to stabilize the skid steering vehicle motion and follow the target yaw rate response, was distributed as traction/braking torque at each tire. The distribution technique was based on a very simple strategy without considering the tire capacity during motion. The effectiveness of the proposed control system was evaluated theoretically using computer simulations and experimentally using a driving simulator. The strategy used by Juyong et al. [11] aimed at minimizing the sum of longitudinal tire forces to find the proper longitudinal tire force distribution. The idea was applied on a skid steering for a robot vehicle with articulated suspension and a maximum speed of 15 km/h.

Based on the foregoing, it is clear that: (i) the most of the work done focused on optimizing the tire usage in longitudinal and lateral direction for the conventional two-wheel steering and (ii) there is an essential need for more researches on the optimal distribution of longitudinal tire forces for skid steering vehicles. Therefore, the objective of this research was to propose a control system to:

- stabilize the motion of skid steering vehicles,
- make the performance of the controlled skid steering vehicle similar to that of conventional one,
- extend the stability limit of skid steering vehicles and allow them to be driven at a relatively high speed.

In order to achieve the aforementioned goals, the exact second order yaw rate response of the conventional two-wheel steering is chosen as a model response for the model following control. The nonlinear sliding control theory is used to calculate the required direct yaw moment by forcing the error between the desired and the actual yaw rate response of the skid steering vehicle to be zero. This yaw moment is required not only to stabilize the skid steering vehicle motion but also to make its handling characteristics close to those of the conventional one. The direct yaw moment is distributed to the four wheels as traction/braking torque using two different strategies. The first one is based on a simple sharing of longitudinal forces among the four wheels whereas the second one is based on the individual ability of each tire to produce longitudinal force using full drive-by-wire system. The effects of the suggested two strategies are investigated and compared using computer simulations program. In addition, both open loop and closed loop evaluations are executed.

2. Nonlinear dynamic model of the skid steering vehicle

This section presents the nonlinear dynamic model of the skid steering vehicle used in this research. The model is described by 9 degrees of freedom. Five degrees are considered for the vehicle body: longitudinal motion, lateral motion, rotation about the z-axis (yaw motion), rotation about the x-axis (roll motion), and rotation about the y-axis (pitch motion), since the main focus of this research was to study the effect of the proposed control system on the skid steering vehicle handling characteristics and not to study the ride comfort. Moreover, the vertical load at each wheel is calculated taking into account the weight shift due to roll and pitch motions as it will be seen later in Section 5.2. Based on this justification, the vertical motion in z direction can be ignored without affecting the simulation results predicted from the proposed dynamic model and related to the handling characteristics. Referring to Fig. 1, the five equations for the vehicle body motion are as follows:

$$\frac{W}{g}(\dot{V}_x - \gamma V_y) + \frac{W_s}{g} h_s \dot{p} = F_{x1} + F_{x2} + F_{x3} + F_{x4} \tag{1}$$

$$\frac{W}{g}(\dot{V}_y + \gamma V_x) - \frac{W_s}{g} h_s \dot{q} = F_{y1} + F_{y2} + F_{y3} + F_{y4} \tag{2}$$

$$I_z \dot{\gamma} + (I_y - I_x) qp = a(F_{y1} + F_{y2}) - b(F_{y3} + F_{y4}) + \frac{t}{2}(F_{x2} + F_{x4} - F_{x3} - F_{x1}) \tag{3}$$

$$I_x \dot{q} + (I_z - I_y)\gamma p - \frac{W_s}{g} h_s (\dot{V}_y + \gamma V_x) = \frac{W_s}{g} h_s g \varphi - K_{roll}\varphi - B_{roll} q \tag{4}$$

$$I_y \dot{p} + (I_x - I_z)\gamma q + \frac{W_s}{g} h_s (\dot{V}_x - \gamma V_y) = \frac{W_s}{g} h_s g \theta - K_{pitch}\theta - B_{pitch} p \tag{5}$$

The remaining four degrees correspond to the dynamics of the four wheels. From Fig. 2, the wheel rotational equation of motion can be written as follows:

$$J_i \frac{d\omega_i}{dt} = T_i - F_{xi} R \tag{6}$$

The longitudinal and lateral friction forces generated at the tires were estimated using the nonlinear tire model described by Abe [12].

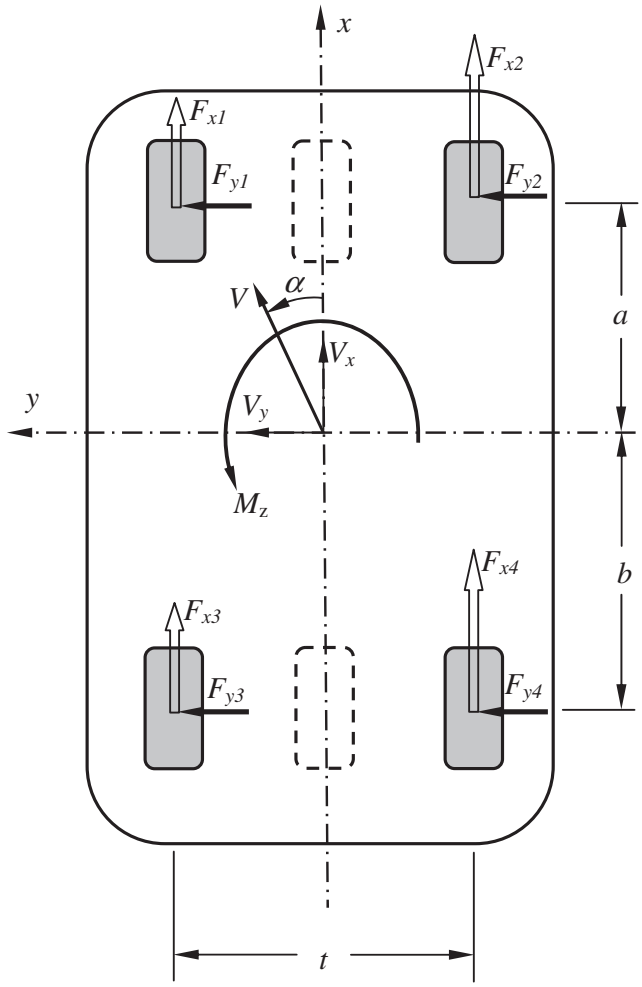

Figure 1 Schematic for the mathematical skid steering vehicle model.

3. Linear dynamics of the skid steering vehicle

Referring to Fig. 1 and following Abe [12], the equations of motion of the 2DOF vehicle planar model with constant speed can be written as follows:

$$\frac{W}{g}V(\dot{\alpha}+\gamma)=F_{yf}+F_{yr} \tag{7}$$

$$I_z\dot{\gamma}=aF_{yf}-bF_{yr}+M_z \tag{8}$$

where

$$F_{yf}=-2C_f\left(\alpha+\frac{a}{V}\gamma\right) \tag{9}$$

$$F_{yr}=-2C_r\left(\alpha-\frac{b}{V}\gamma\right) \tag{10}$$

Substituting Eqs. (9) and (10) into Eqs. (7) and (8) yields

$$\frac{W}{g}V\dot{\alpha}+2(C_f+C_r)\alpha+\left[\frac{W}{g}V+\frac{2}{V}(aC_f-bC_r)\right]\gamma=0 \tag{11}$$

$$2(aC_f-bC_r)\alpha+I_z\dot{\gamma}+2\frac{\gamma}{V}(a^2C_f+b^2C_r)=M_z \tag{12}$$

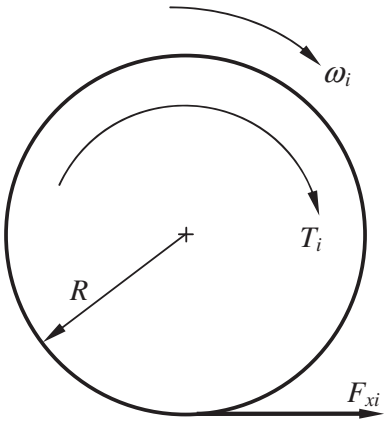

Figure 2 Wheel rotation and torques.

Eqs. (11) and (12) can be written in matrix form as follows:

$$\begin{bmatrix}\frac{W}{g}Vs+2(C_f+C_r) & \frac{W}{g}V+\frac{2}{V}(aC_f-bC_r)\\ 2(aC_f-bC_r) & I_zs+\frac{2}{V}(a^2C_f+b^2C_r)\end{bmatrix}\begin{bmatrix}\alpha(s)\\ \gamma(s)\end{bmatrix}=\begin{bmatrix}0\\ M_Z\end{bmatrix}$$

From the above matrix form, the steady state yaw rate response of the skid steering vehicle can be expressed as follows:

$$\gamma_{ss}=\left(\frac{1}{1-\frac{W}{g}\frac{V^2}{2(a+b)^2}\frac{(aC_f-bC_r)}{C_fC_r}}\right)\frac{V}{(a+b)}\frac{(C_f+C_r)}{2C_fC_r(a+b)}M_z \tag{13}$$

Abe [12] presented the steady state yaw rate response of the conventional two-wheel steering vehicle as follows:

$$\gamma_{ss}=\left(\frac{1}{1-\frac{W}{g}\frac{V^2}{2(a+b)^2}\frac{(aC_f-bC_r)}{C_fC_r}}\right)\frac{V}{(a+b)}\frac{\psi}{r} \tag{14}$$

Comparing Eqs. (13) and (14), an expression of the direct yaw moment needed to steer the uncontrolled skid steering vehicle can be obtained as follows:

$$M_z=\frac{2C_fC_r(a+b)}{C_f+C_r}\frac{\psi}{r} \tag{15}$$

4. Control method

4.1. Model response

The handling characteristics of a skid steering vehicle are different from those of a conventional two-wheel steering vehicle due to the over steer characteristics of the first. The motion of a skid steering vehicle becomes unstable when it reaches a specific speed. Indeed, driving a conventional two-wheel steering vehicle is convenient to the most of the drivers. Therefore, the yaw rate response of the 2DOF linear plane model of the conventional two-wheel steering vehicle is considered as model response for the model following control theory. It was adopted in order to stabilize the motion of skid steering vehicle and make its handling characteristics close to those of conventional one. The model response of yaw rate was written by Abe [12] as follows:

$$\frac{\gamma r}{\psi} = G_R \frac{1 + T_r s}{1 + \frac{2\zeta}{\omega_n} s + \frac{1}{\omega_n^2} s^2} \tag{16}$$

where

$$G_R = \frac{1}{1 + AV^2}\left(\frac{V}{a+b}\right)$$

$$T_r = \frac{\frac{W}{g} aV}{2(a+b)C_r}$$

$$\zeta = \frac{\frac{W}{g}(a^2 C_f + b^2 C_r) + I_z(C_f + C_r)}{2(a+b)\sqrt{\frac{W}{g} I_z C_f C_r (1 + AV^2)}}$$

$$\omega_n = \frac{2(a+b)}{V}\sqrt{\frac{C_f C_r}{\frac{W}{g} I_z}}\sqrt{1 + AV^2}$$

$$A = \frac{\frac{W}{g}}{2(a+b)^2}\left(\frac{bC_r - aC_f}{C_f C_r}\right)$$

4.2. Control law of the direct yaw moment

The nonlinear sliding control theory presented by Jean-Jacques and Weiping [13] was used to calculate the required direct yaw moment needed to steer the skid steering vehicle and stabilize its motion. Accordingly, the sliding surface S can be defined as follows:

$$S = \gamma - \gamma_t = 0 \tag{17}$$

Eq. (17) states that the difference between the yaw rate response of the skid steering vehicle and that of the conventional two-wheel steering is converged to zero. In other words, the yaw rate response of the skid steering vehicle is forced to follow that of the conventional vehicle. The sliding condition is as follows:

$$\dot{S} + kS = 0 \tag{18}$$

Substituting Eq. (16) into Eq. (17), and then substituting the resultant equation into Eq. (18) the following equation can be obtained:

$$\dot{\gamma} + k\gamma - G_R \frac{1 + T_r s}{1 + \frac{2\zeta}{\omega_n} s + \frac{1}{\omega_n^2} s^2}\left(\frac{\dot{\psi} + k\psi}{r}\right) = 0 \tag{19}$$

And, from Fig. 1, the equation of yaw motion is

$$I_z \dot{\gamma} = 2(aF_{yf}^* - bF_{yr}^*) + M_Z \tag{20}$$

From Eqs. (19) and (20), the control law of the direct yaw moment can be formulated as follows:

$$M_z = 2(bF_{yr}^* - aF_{yf}^*) - k\gamma I_z + G_R I_z \frac{1 + T_r s}{1 + \frac{2\zeta}{\omega_n} s + \frac{1}{\omega_n^2} s^2}\left(\frac{\dot{\psi} + k\psi}{r}\right) \tag{21}$$

The lateral forces (F_{yf}^* and F_{yr}^*) generated by front and rear wheels were estimated using the simple tire model presented by Abe et al. [14].

5. Determination of traction/braking torque

The direct yaw moment given by Eq. (21) is distributed to the four wheels as wheel longitudinal forces. Then, the traction/braking torque that should be applied at each wheel in order to follow the desired yaw rate response and also stabilize the skid steering vehicle motion is calculated. In this paper, an independent distribution of wheel longitudinal forces is proposed and compared to the simple distribution method.

5.1. Simple distribution method

In the simple distribution method, the direct yaw moment is distributed to front and rear axles in such a way that the distribution ratio is constant as follows:

$$M_{Zf} = drM_z \tag{22}$$

$$M_{Zr} = (1 - dr)M_z \tag{23}$$

Meanwhile, the right and left wheels on front/rear axles bear the same amount of traction/braking force. As a result, the traction/braking torque on each wheel can be calculated as follows:

$$T_1 = T_2 = M_{zf}\frac{R}{t} \tag{24}$$

$$T_3 = T_4 = M_{zr}\frac{R}{t} \tag{25}$$

5.2. Independent distribution method

In the simple distribution method presented above, the direct yaw moment was distributed to the four wheels without taking into account the ability of each wheel to produce the required longitudinal force. Therefore, the main objective of the independent distribution method proposed in this paper was to figure out how much traction/braking torque should be applied at each wheel to: (a) steer the skid steering vehicle, (b) stabilize the skid steering vehicle lateral motion, and finally (c) force the skid steering vehicle yaw rate to follow the desired yaw rate response. From the concept of friction circle, the traction/braking force acting on a wheel is proportional to its vertical load. Accordingly, the sum of squared normalized longitudinal forces produced at the four wheels is adopted as the objective function for the proposed independent distribution technique.

$$\mu = \frac{F_{x1}^{*2}}{F_{z1}^2} + \frac{F_{x2}^{*2}}{F_{z2}^2} + \frac{F_{x3}^{*2}}{F_{z3}^2} + \frac{F_{x4}^{*2}}{F_{z4}^2} \tag{26}$$

The independent distribution of F_{x1-4}^* is obtained by minimizing the objective function μ taking into account the following constraints: (a) the direct yaw moment must be equal to the yaw moment produced by the longitudinal forces of wheels, Eq. (27) and (b) the total longitudinal force following the driver's command must be equal to the sum of longitudinal forces produced by the four wheels, Eq. (28).

$$M_z = \frac{t}{2}(F_{x2}^* - F_{x1}^* + F_{x4}^* - F_{x3}^*) \tag{27}$$

$$\frac{W}{g} a_{xdes} = F_{x1}^* + F_{x2}^* + F_{x3}^* + F_{x4}^* \tag{28}$$

The equality constraints presented in Eqs. (27) and (28) can be used to eliminate two of the four variables in the objective function given by Eq. (26). From Eqs. (27) and (28), the following relations can be obtained:

$$F_{x4}^{*} = \frac{W}{g} a_{xdes} - F_{x1}^{*} - F_{x2}^{*} - F_{x3}^{*} \tag{29}$$

$$F_{x3}^{*} = \frac{W}{2g} a_{xdes} - F_{x1}^{*} - \frac{M_z}{t} \tag{30}$$

Substituting the above expression into Eq. (26), the new objective function of two variables F_{x1}^{*} and F_{x2}^{*} is obtained

$$\mu = \frac{F_{x1}^{*2}}{F_{z1}^{2}} + \frac{F_{x2}^{*2}}{F_{z2}^{2}} + \frac{1}{F_{z3}^{2}} \left(\frac{W}{2g} a_{xdes} - F_{x1}^{*} - \frac{M_z}{t} \right)^2 + \frac{1}{F_{z4}^{2}} \left(\frac{W}{2g} a_{xdes} - F_{x2}^{*} + \frac{M_z}{t} \right)^2 \tag{31}$$

The expressions of F_{x1}^{*} and F_{x2}^{*} can be determined using the following minimizing conditions:

$$\frac{\partial \mu}{\partial F_{x1}^{*}} = 2\frac{F_{x1}^{*}}{F_{z1}^{2}} - \frac{2}{F_{z3}^{2}} \left(\frac{W}{2g} a_{xdes} - F_{x1}^{*} - \frac{M_z}{t} \right) = 0$$

$$F_{x1}^{*} = \frac{\frac{W}{g}\frac{a_{xdes}}{F_{z3}^{2}} - \frac{2M_z}{tF_{z3}^{2}}}{\frac{2}{F_{z1}^{2}} + \frac{2}{F_{z3}^{2}}} \tag{32}$$

$$\frac{\partial \mu}{\partial F_{x2}^{*}} = 2\frac{F_{x2}^{*}}{F_{z2}^{2}} - \frac{2}{F_{z4}^{2}} \left(\frac{W}{2g} a_{xdes} - F_{x2}^{*} + \frac{M_z}{t} \right) = 0$$

$$F_{x2}^{*} = \frac{\frac{W}{g}\frac{a_{xdes}}{F_{z4}^{2}} + \frac{2M_z}{tF_{z4}^{2}}}{\frac{2}{F_{z2}^{2}} + \frac{2}{F_{z4}^{2}}} \tag{33}$$

Once the wheel longitudinal force is obtained, the traction/braking torque that should be applied at each wheel in the full drive-by-wire system is given by the following:

$$T_i = RF_{xi}^{*} \quad (i = 1 - 4) \tag{34}$$

It is noticed that the independent distribution technique depends on the wheel vertical load, F_{zi}. Therefore, it is essential to estimate the vertical load at each wheel by taking into account the effect of load shift due to roll and pitch motions. The load shift can be estimated by measuring both the longitudinal and lateral acceleration of the vehicle. The estimated vertical loads at the four wheels are obtained as follows:

$$F_{z1} = \frac{Wb}{2(a+b)} - \frac{W_s}{g}\frac{a_x h_s}{2(a+b)} - k_f \frac{W_s}{g}\frac{a_y h_s}{t} \tag{34}$$

$$F_{z2} = \frac{Wb}{2(a+b)} - \frac{W_s}{g}\frac{a_x h_s}{2(a+b)} + k_f \frac{W_s}{g}\frac{a_y h_s}{t} \tag{35}$$

$$F_{z3} = \frac{Wa}{2(a+b)} + \frac{W_s}{g}\frac{a_x h_s}{2(a+b)} - k_r \frac{W_s}{g}\frac{a_y h_s}{t} \tag{36}$$

$$F_{z4} = \frac{Wa}{2(a+b)} + \frac{W_s}{g}\frac{a_x h_s}{2(a+b)} + k_r \frac{W_s}{g}\frac{a_y h_s}{t} \tag{37}$$

The block diagram presented in Fig. 3 summarizes the proposed control system.

6. Simulation results and discussion

The dynamic model of the skid steering vehicle (SSV) described in Section 2 was simulated using Matlab/Simulink software. The influence of the proposed independent distribution method (ID) was investigated through both open loop and closed loop tests. Small passenger car with data as shown in Table 1, Appendix A, was used in the computer simulations. In the closed loop test, the simple first order preview model described by Mokhiamar and Abe [7] modeled the driver. In this model, the driver steered the steering wheel in such way to eliminate the difference between the target path and the vehicle position look-ahead distance. The geometry of the target path is shown in Fig. 4. On the other hand, in case of open loop test, the driver steered the steering wheel with a specific and prescribed steering input that did not change during the simulation regardless of the vehicle response. Moreover, the handling performance of the skid steering vehicle of the proposed control system (SSV/ID) is compared with (a) the performance of skid steering vehicle without control (SSV/NC); (b) the performance of controlled skid steering vehicle based on the simple distribution method (SSV/SD); and (c) the handling characteristics of the conventional two-wheel steering vehicle (CFWSV).

The SSV/SD response had been evaluated for various values of *dr* and the most acceptable response was found when *dr* equals to 0.5. As a first phase of this research, the vehicle speed was maintained constant during the tests. In other words, the foot-brake pressure provided by the driver was equal to zero, whereas the acceleration pedal pressure is constant. The vehicle running speed was equal to 30 m/s and the tests were executed on dry road condition.

The results obtained using the simulations program are illustrated in Figs. 5–13. In all these figures, there are two sub-figures: sub-figure (a) corresponds to open loop test, whereas sub-figure (b) corresponds to closed loop test. Fig. 5 shows the steering wheel angle provided by the driver. Of course, in case of open loop test, there is only one plot for all the cases treated in this paper. On the other hand, in case of closed loop test, there are four different plots one for each case. Clearly, skid steering vehicles without control, for which M_z is calculated using Eq. (15), have unstable motion. However, each of the proposed systems allows achieving stable motion. In addition, there is a good matching between the handling performance of the controlled skid steering vehicle and the performance of the conventional two-wheel steering vehicle. The yaw rate, the vehicle sideslip angle and the lateral acceleration responses are illustrated in Figs. 6–8. Once again, both the simple and the independent distribution methods resulted in a stable motion. Moreover, the proposed control method produces desirable vehicle responses when compared with the target yaw rate response and the response of the conventional vehicle. It is noteworthy that at such a high speed, the uncontrolled SSV shows unstable motion. This is mainly because the stabilizing yaw moment generated by the wheel lateral forces could not balance the yaw moment, M_z, generated by the wheel longitudinal forces and eventually the vehicle falls into an over steering state. Therefore, there is an essential need to control the value of the input direct yaw moment in order to stabilize the SSV motion.

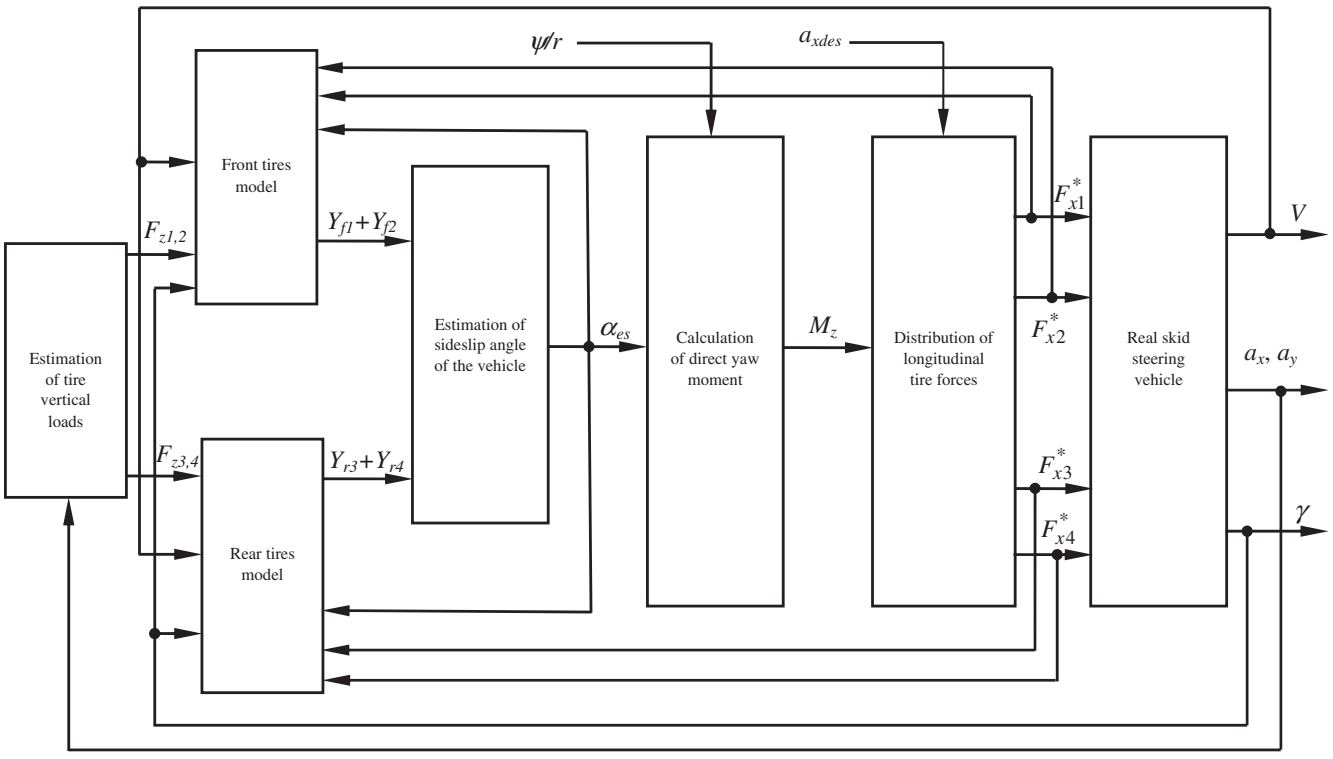

Figure 3 Block diagram of the proposed control systems.

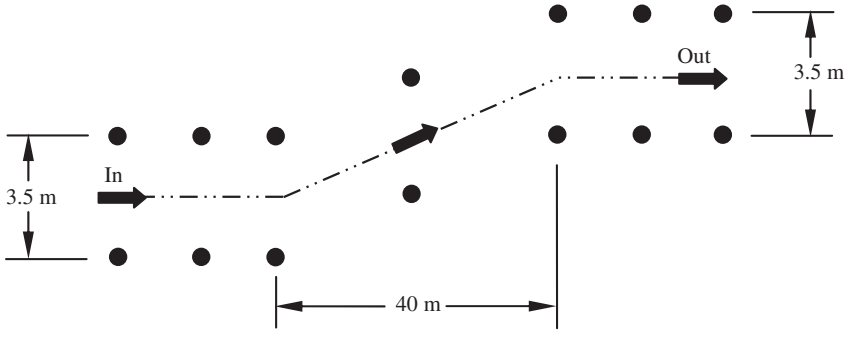

Figure 4 Geometry of the single lane change task.

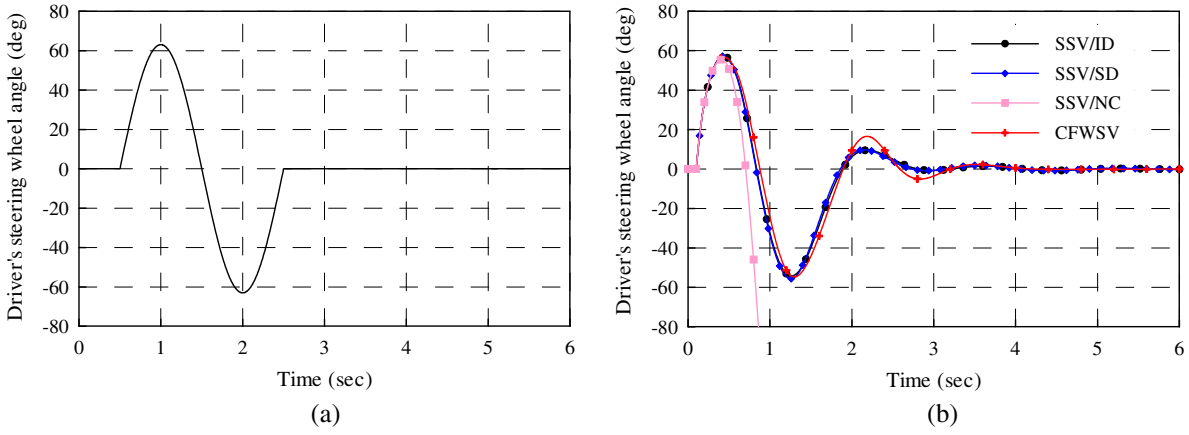

Figure 5 Driver steering wheel input time history (dry road, $V = 30$ m/s): (a) open loop evaluation, and (b) closed loop evaluation.

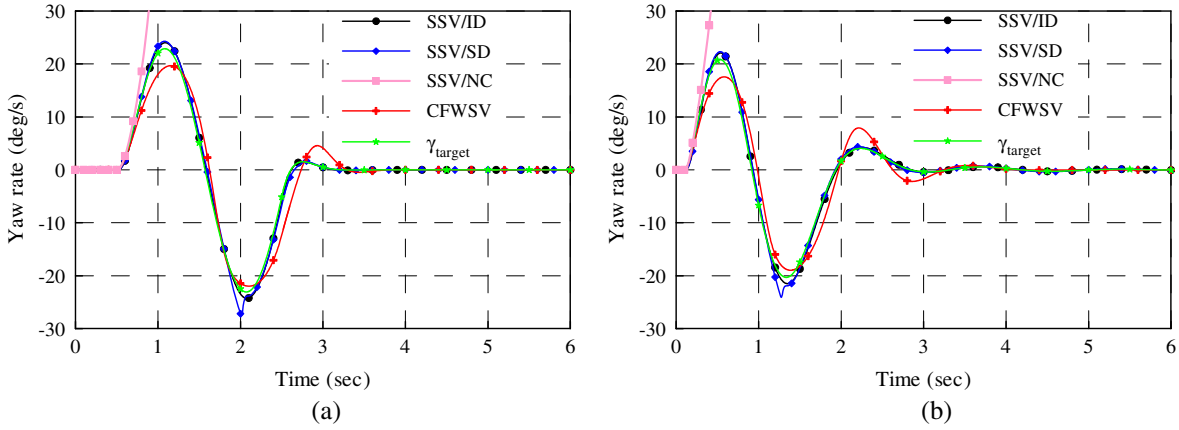

Figure 6 Comparison of vehicle yaw rate response (dry road, $V = 30$ m/s): (a) open loop evaluation, and (b) closed loop evaluation.

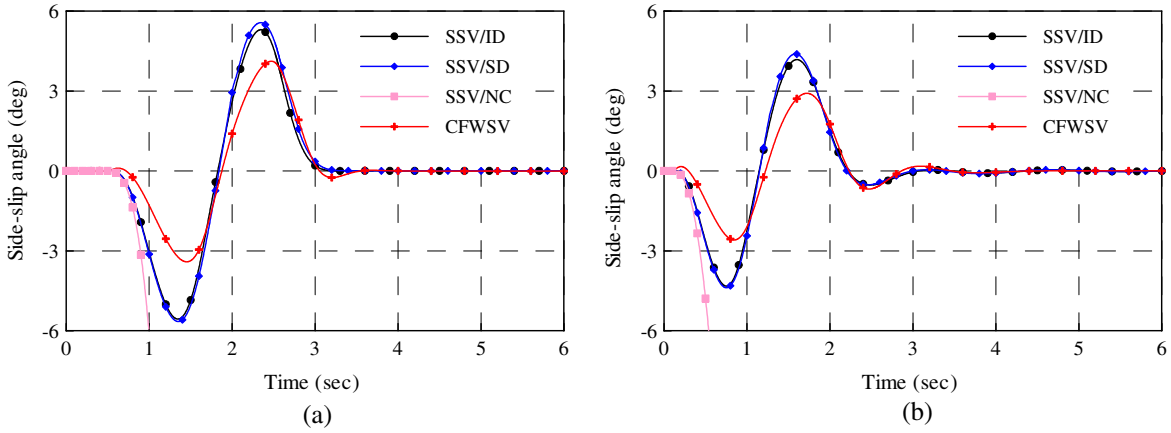

Figure 7 Comparison of vehicle sideslip angle response (dry road, $V = 30$ m/s): (a) open loop evaluation, and (b) closed loop evaluation.

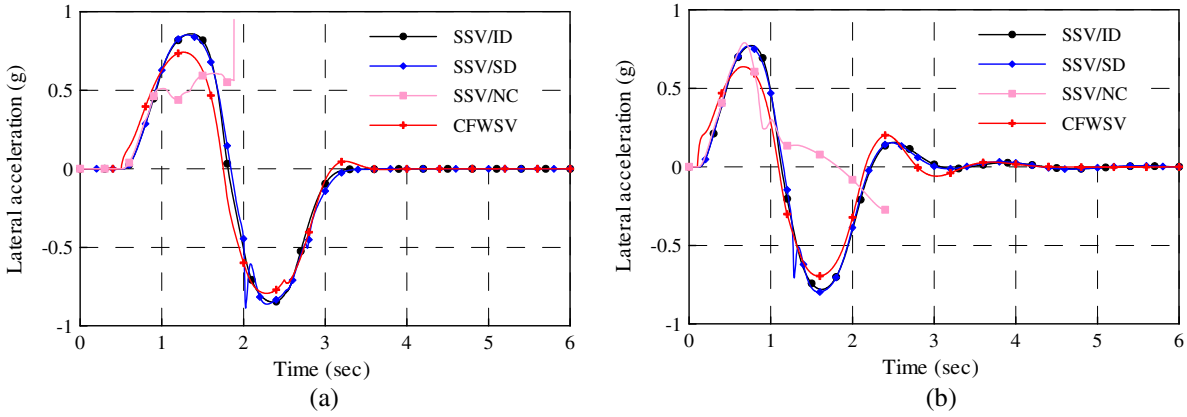

Figure 8 Comparison of vehicle lateral acceleration response (dry road, $V = 30$ m/s): (a) open loop evaluation, and (b) closed loop evaluation.

Regarding the difference between the controlled skid steering vehicle based on simple distribution and independent distribution methods, it can be said that both methods control the motion of SSV. However, the SSV with independent distribution shows a better response compared to simple distribution method. The evidence of good matching between controlled SSV and CFWSV performances is also clearly spotted in Figs. 6–8. In addition, the matching in case of SSV/ID is

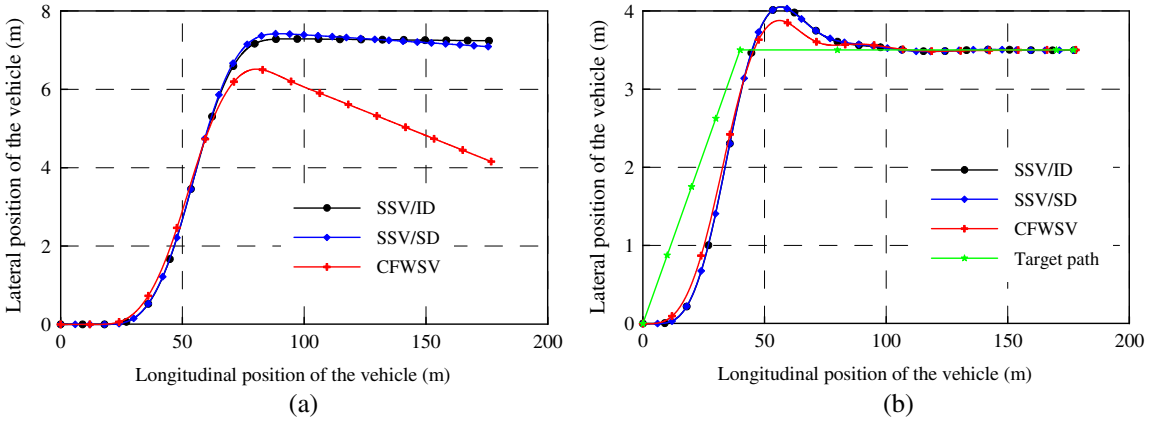

Figure 9 Vehicle trajectory (dry road, $V = 30$ m/s): (a) open loop evaluation, and (b) closed loop evaluation.

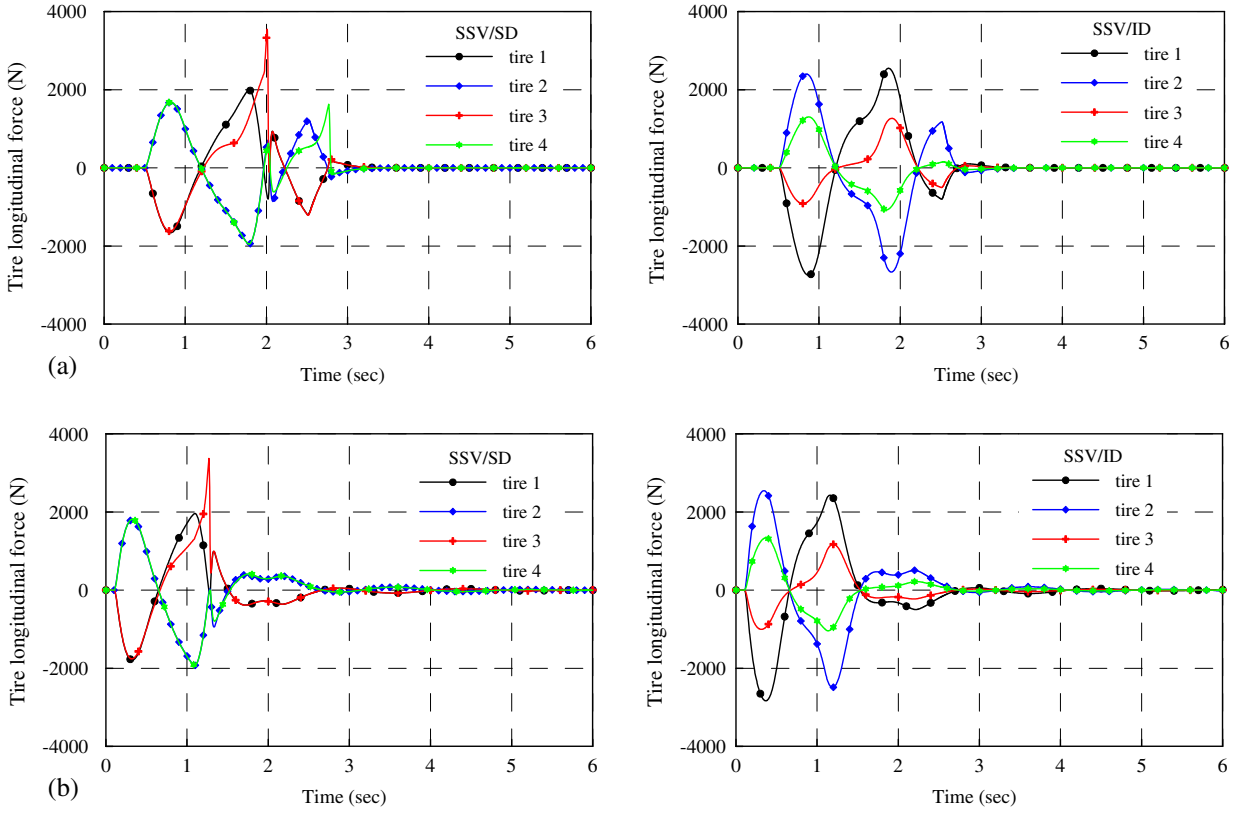

Figure 10 Time history of the tires' longitudinal forces (dry road, $V = 30$ m/s): (a) open loop evaluation, and (b) closed loop evaluation.

better than in case of SSV/SD. The trajectories of controlled SSV and CFSWV are compared in Fig. 9. In the closed loop test, Fig. 9(b), the initial condition of the longitudinal position of the vehicle is set to zero in order to force the driver to apply a sudden steering in order to simulate the case of severe evasive lane change. This explains the relatively large difference between the actual vehicle position and the target path especially at the beginning of the maneuvering. The presented results show a significant effect of the proposed control system on the trajectory of SSV.

Going deep inside the SSV dynamics, Figs. 10–13 are provided in order to understand and analyze the difference between the proposed independent longitudinal force distribution method and the simple one. Fig. 10 shows the longitudinal force at each wheel due to the traction/braking torque calculated from Eqs. (24) and (25)/or (34). Fig. 10(a), corresponding to open loop test, has two sub-figures: one for SSV/SD and another for SSV/ID. It is obvious that the SSV/ID utilizes the ability of each wheel properly in coordination with its capacity since the ability of the wheel to produce force depends

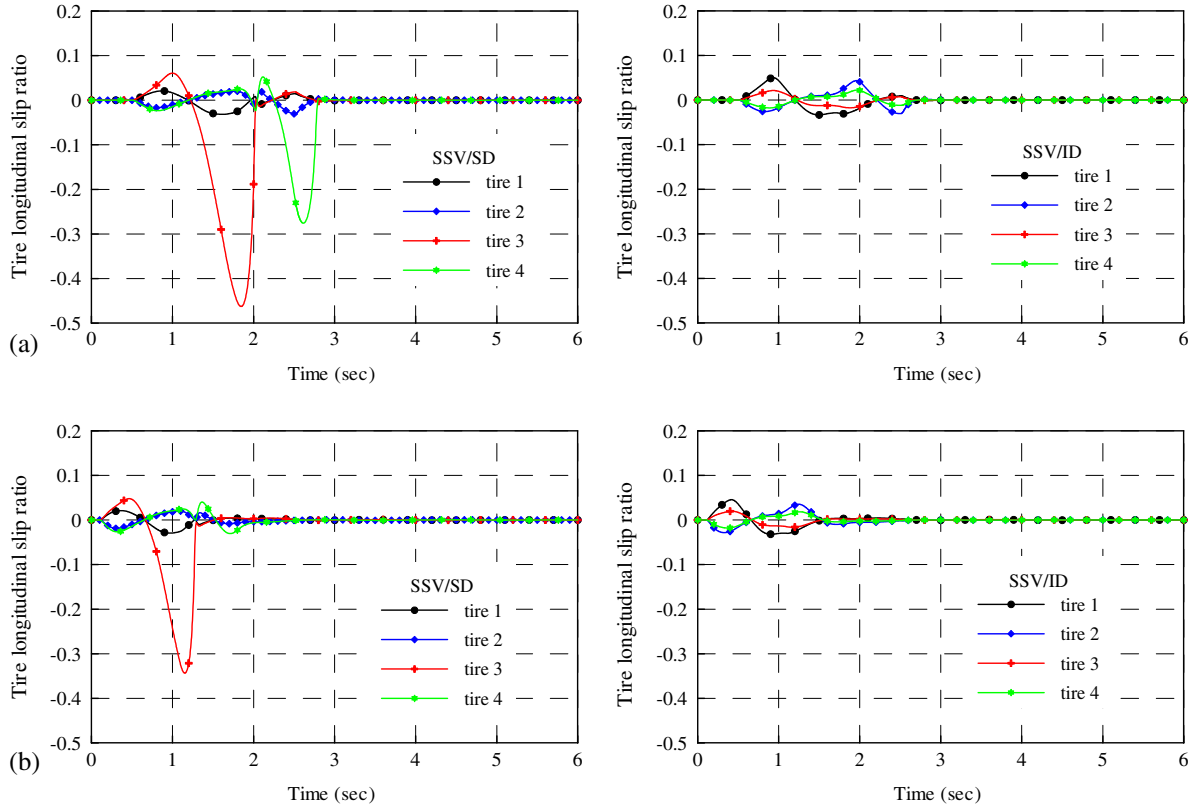

Figure 11 Time history of the tires' longitudinal slip ratio (dry road, $V = 30$ m/s): (a) open loop evaluation, and (b) closed loop evaluation.

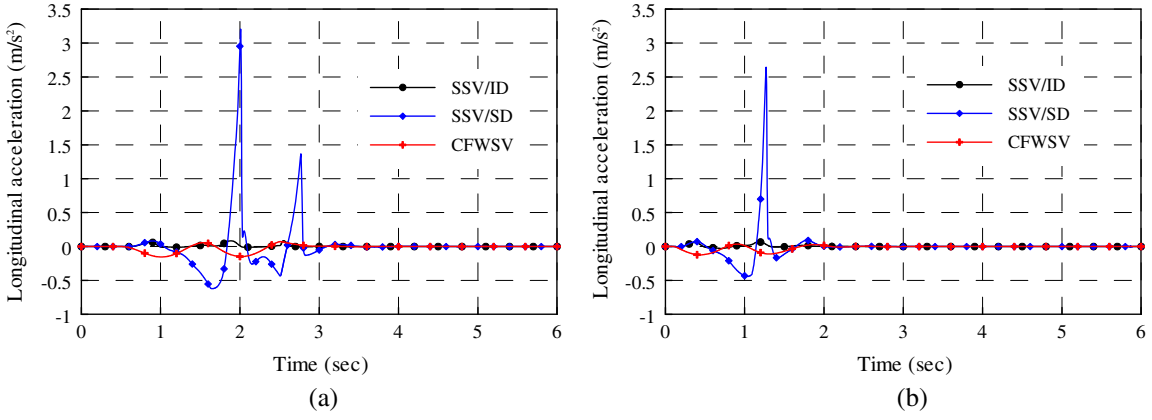

Figure 12 Comparison of the longitudinal acceleration of the vehicle (dry road, $V = 30$ m/s): (a) open loop evaluation, and (b) closed loop evaluation.

on the vertical load applied on it. On the other hand, an illogical time history is presented in the case of SSV/SD. Definitely, this will affect the longitudinal slip ratio of the four wheels as shown in Fig. 11. It should be noted from this figure that in case of SSV/SD, the longitudinal slip of wheels 3 and 4 exceeds −0.3. The negative sign appears since the wheels are subjected to a traction torque produced by a positive longitudinal force as already shown in Fig. 10. This means that the ability of these wheels to produce longitudinal force decreases. Moreover, these wheels may lock if an extra traction torque is required. On the other hand, the maximum value of the wheel longitudinal slip among the four wheels in case of SSV/ID is less than ± 0.05. This will necessarily have an impact on the longitudinal dynamics of the SSV as shown in Fig. 12. On the other hand, the SSV/ID has a very reasonable longitudinal dynamics as well as a performance very close to that of the conventional two-wheel steering vehicle. On the contrary, SSV/SD shows unacceptable longitudinal dynamics. Finally,

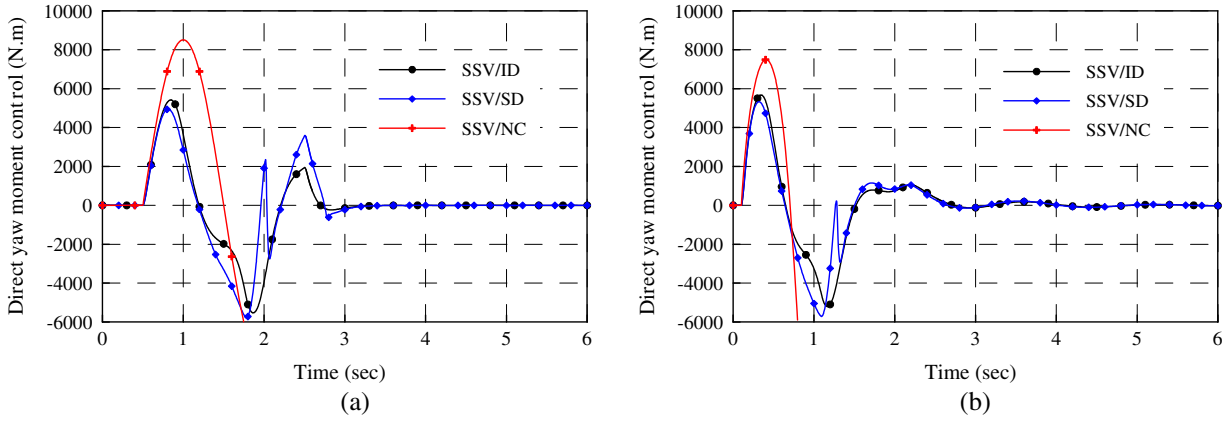

Figure 13 Comparison of direct yaw moment control (dry road, $V = 30$ m/s): (a) open loop evaluation, and (b) closed loop evaluation.

Fig. 13 depicts the time history of the direct yaw moment for uncontrolled SSV and controlled SSV with the proposed two distribution techniques. As illustrated in this figure, unstable motion is predicted for the uncontrolled SSV, while smooth and acceptable direct yaw moment (without large fluctuation) is predicted in case of controlled SSV with independent distribution technique.

7. Summary and conclusions

In this paper, an independent distribution technique of wheel longitudinal forces taking into account the ability of the wheels to produce individual friction force based on full drive-by-wire system was proposed. A distribution method based on a simple strategy was presented for the sake of comparison. The control methods aimed at stabilizing the motion of skid steering vehicles at high speed and forcing the yaw rate response of the skid sheering vehicle to follow the yaw response of the conventional two-wheel steering vehicle. Simulations program of the comprehensive nonlinear dynamic model of the skid steering vehicle were used to investigate the effectiveness of the suggested controllers. Vehicle responses to both open and closed loop tests were studied. As a first phase of this research work, the simulations were executed assuming that the skid steering vehicle runs at constant speed.

The simulation results showed that both proposed distribution methods increased the stability limit of skid steering vehicles at relatively high speed. In addition, the methods allowed letting the yaw rate response of such vehicles follow the desired one. However, skid steering vehicles with independent distribution technique showed better and more acceptable longitudinal dynamics. Finally, it can be said that the proposed independent distribution technique, if implemented in off-road vehicles that install wheels with high performance, opens new insights to run skid steering vehicles at relatively high speeds. In addition, it allows generating stable motion and reasonable handling characteristics for common drivers.

Appendix A

See Table 1.

Table 1 Parameters of skid steering vehicle.

Parameter	Value	Unit
a	1.0	m
b	1.5	m
C_f, C_r	62,760	N/rad
B_{pitch}	12,950	N ms/rad
B_{roll}	4402	N ms/rad
h_s	0.52	m
I_x	500	kg m^2
I_y	2300	kg m^2
I_z	2200	kg m^2
J_i	1.2	kg m^2
K_{pitch}	140,000	N m/rad
K_{roll}	88,327	N m/rad
R	0.3	m
t	1.46	m
W	13,500	N
W_S	12,300	N

References

[1] Y. Suzuki, Y. Kano, M. Abe, A study on tyre force distribution controls for full drive-by-wire electric vehicle, Veh. Syst. Dynam. 52 (4) (2014) 235–250.
[2] A. Goodarzi, M. Mohammadi, Stability enhancement and fuel economy of the 4-wheel-drive hybrid electric vehicles by optimal tyre force distribution, Veh. Syst. Dynam. 52 (4) (2014) 539–561.
[3] CC. Wang, SY. Cheng, T. Hsiao, WY. Chou, Application of optimum tire force distribution to vehicle motion control, in: IEEE/ASME International Conference on Advanced Intelligent Mechatronics, Kaohsiung, Taiwan, 2012, pp. 538–543.
[4] S.H. Kim, D.H. Kim, C.J. Kim, M.A. Ali, S.H. Back, C.S. Han, A study on the improvement of the tire force distribution method for rear wheel drive electric vehicle with in-wheel motor, in: IEEE/SICE International Symposium on System Integration, Fukuoka, Japan, 2012, pp. 390–395.
[5] M. Naraghi, A. Roshanbin, A. Tavasoli, Vehicle stability enhancement – an adaptive optimal approach to the distribution of tyre forces, Proc. IMechE Part D: J. Automob. Eng. 224 (4) (2010) 443–453.
[6] O. Mokhiamar, Stabilization of car-caravan combination using independent steer and drive/or brake forces distribution, Alexandria Eng. J. 54 (2015) 315–324.

[7] O. Mokhiamar, M. Abe, Simultaneous optimal distribution of lateral and longitudinal tire forces for the model following control, Trans. ASME J. Dynam. Syst. Meas. Control 126 (2004) 753–763.
[8] E. Ono, Y. Hattori, Y. Muragishi, K. Koibuchi, Vehicle dynamics integrated control for four-wheel-distributed steering and four-wheel-distributed traction/braking systems, Veh. Syst. Dynam. 44 (2) (2006) 139–151.
[9] H. Sasaki, M. Abe, Behavior analysis of skid steer control vehicles, in: Proceeding of International Federation of Automatic Control symposium on advances in automotive control, Italy, 2004, pp. 727–732.
[10] H. Sasaki, M. Abe, Analysis of controlled skid steer vehicle, in: Proceeding of International Symposium on Advanced Vehicle Control, Han University Arnhem, Netherlands, 2004, pp. 827–832.
[11] K. Juyong, K. Wongun, J. Soungyong, Y. Kyongsu, Skid steering based trajectory tracking controller of robotic vehicle with articulated suspension, in: Proceeding of International Symposium on Advanced Vehicle Control, Kobe, Japan, 2008, pp. 559–564.
[12] M. Abe, Vehicle Handling Dynamics, Theory and Application, first ed., Elsevier Ltd, 2009.
[13] E.S. Jean-Jacques, L. Weiping, Applied nonlinear control, Prentice-Hall, Englewood Cliffs, New Jersey, 1991.
[14] M. Abe, A. Kato, K. Suzuki, Y. Kano, Estimation of vehicle side-slip angle for DYC by using on-board–tire-model, in: Proceeding of International Symposium on Advanced Vehicle Control, Nagoya, Japan, 1998, pp. 437–442.